

33. For densities of Phobos, see G. A. Avensov *et al.*, *Planet. Space Sci.* **39**, 281 (1991); for Deimos, B. G. Williams *et al.*, *Proc. Lunar Planet. Sci. Conf.* **19**, 1274 (1988). Note that D. E. Smith *et al.* [*Geophys. Res. Lett.* **22**, 2171 (1995)] calculated a density of 1.5 g/cm³ for Phobos.
34. R. Millis *et al.*, *Icarus* **72**, 502 (1987).
35. E. Asphaug and H. J. Melosh, *ibid.* **101**, 144 (1993); S. G. Love and T. J. Ahrens, *ibid.* **124**, 141 (1996).
36. E. Asphaug *et al.*, *ibid.* **120**, 158 (1996).
37. R. Greenberg *et al.*, *ibid.*, p. 106.
38. M. J. S. Belton *et al.*, *Nature* **374**, 785 (1995).
39. A. W. Harris, *Icarus* **107**, 209 (1994); R. P. Binzel, *ibid.* **63**, 99 (1985); A. W. Harris, *Bull. Am. Astron. Soc.* **15**, 828 (1983).
40. R. P. Binzel *et al.*, in *Asteroids II*, P. Binzel *et al.*, Eds. (Univ. of Arizona Press, Tucson, 1989), pp. 416–441.
41. C. R. Chapman *et al.*, *Nature* **374**, 783 (1995); J. Veverka *et al.*, *Icarus* **120**, 200 (1996).
42. P. D. Hamilton and J. A. Burns, *Icarus* **92**, 118 (1991).
43. P. C. Thomas *et al.*, *J. Geophys. Res.* **86**, 8675 (1981).
44. P. C. Thomas *et al.*, *Science* **277**, 1492 (1997).
45. S. Croft, *Icarus* **99**, 402 (1992).
46. P. C. Thomas *et al.*, *ibid.* **107**, 23 (1994).
47. P. Geissler *et al.*, *ibid.* **120**, 140 (1996).
48. This contribution is dedicated to the memory of Jürgen Rahe and Eugene Shoemaker, who played key roles in making the exploration of asteroids a reality. Both were involved in the studies that led to the initiation of the NEAR Project. Rahe, in his role as Science Program Director for Solar System Exploration, oversaw the activities of the project until his tragic death shortly before the Mathilde encounter. Shoemaker

participated in the Mathilde encounter activities as a guest of the NEAR Imaging Team. We are grateful to D. Yeomans of NEAR's Radio Science Team for close collaboration in the determination of Mathilde's density, to two reviewers for helpful comments, and to B. Chew, who paid close attention to the preparation of the manuscript. We are especially indebted to the Mission Design, Mission Operations, and Flight teams at the Applied Physics Laboratory, and to the Navigation Team at the Jet Propulsion Laboratory. Special thanks are due to G. Heyler, M. Holdridge, A. Santo, W. Owen, J. Miller, D. Scheeres, B. G. Williams, D. Dunham, D. Morrison, A. Harris, C. Porco, C. Shoemaker, F. Vilas, A. Rivkin, R. Binzel, P. Helfenstein, C. Tector, and M. Roth.

19 September 1997; accepted 19 November 1997

Quantum-Confined Stark Effect in Single CdSe Nanocrystallite Quantum Dots

S. A. Empedocles and M. G. Bawendi*

The quantum-confined Stark effect in single cadmium selenide (CdSe) nanocrystallite quantum dots was studied. The electric field dependence of the single-dot spectrum is characterized by a highly polarizable excited state ($\sim 10^5$ cubic angstroms, compared to typical molecular values of order 10 to 100 cubic angstroms), in the presence of randomly oriented local electric fields that change over time. These local fields result in spontaneous spectral diffusion and contribute to ensemble inhomogeneous broadening. Stark shifts of the lowest excited state more than two orders of magnitude larger than the linewidth were observed, suggesting the potential use of these dots in electro-optic modulation devices.

Optical switches are a key component in many optical computing and fiber-optic communication designs. In particular, devices based on the quantum-confined Stark effect (QCSE) in quantum wells (QWs) have proven useful in many optical modulation applications (1). In these devices, quantum confinement in one dimension allows the formation of excitonic states with electric field induced Stark shifts many times greater than the electron-hole binding energy (1). As a result, the Stark effect in QWs is significantly enhanced relative to that in bulk materials. Quantum dots (QDs), the zero-dimensional analog of QWs, represent the ultimate in semiconductor-based quantum-confined systems (2). Narrow transition linewidths inherent in QDs (3–5), coupled with large Stark shifts, should result in electro-optic modulation devices with even greater efficiency.

Nanocrystallite QDs synthesized as colloids are a particularly flexible material for such QD heterostructures. In particular, CdSe nanocrystallite QDs, with a band gap tunable throughout the visible range, have been extensively studied as a prototypical

QD system. These dots can be synthesized in macroscopic quantities with diameters that are tunable during synthesis (6). They are easily incorporated into a variety of insulating and conducting polymers as well as thin films of bulk semiconductors (7). They can also be manipulated into close-packed glassy thin films (8) and ordered three-dimensional arrays (9).

In addition to possible device applications, the QCSE can be used to probe the nature of the excited states in QDs. Delocalized exciton states within the QD core should be highly polarizable, whereas localized surface trap states should have a strong dipole character. Spectral broadening, due to structural and environmental inhomogeneities, has generally complicated the interpretation of ensemble optical studies, including Stark measurements. For example, although the presence of an excited-state dipole has been suggested in ensemble Stark absorption studies (10), nearly identical Stark data have also been interpreted without the need for a polar state (11).

The elimination of inhomogeneous broadening through single QD spectroscopy has allowed many fundamental observations in recent years (3–5, 12–14). In this report, we use fluorescence microscopy to study the QCSE in single CdSe nanocrystallite QDs of varying sizes.

tallite QDs of varying sizes.

Five sample sizes were studied. The QDs were synthesized as in (6), with average radii of 22, 24, 26, 29, and 37.5 Å. The 37.5 Å sample was further divided, and half of the sample was overcoated with a ~ 6 Å layer of ZnS (15). The 24 Å sample was also overcoated with ZnS. We applied electric fields by using photolithographically patterned Ti-Au electrodes on a crystalline quartz substrate. The electrodes were patterned in an interdigitated design with an interelectrode spacing of 5 μm and a height of 1200 Å. A dilute solution of QDs in hexane was placed over the electrodes and was immediately wicked from the surface, leaving only a small number of dots adsorbed to the substrate. Spectra were taken from dots located midway between adjacent electrodes to ensure a uniform electric field (16). We took single dot spectra at 10 K using a far-field epifluorescence microscope [described elsewhere (3)] with 514-nm excitation from an Ar⁺ laser.

In a series of emission spectra taken from the same single dot with the applied electric field either on or off (Fig. 1A), a single peak corresponding to the zero phonon line (ZPL) can be observed shifting between two distinct energies in response to the field. This shift is highly reproducible and results in a change in energy that is 15 times greater than the observed, resolution-limited linewidth and more than two orders of magnitude greater than the linewidths previously reported for the emitting state (3). Although the first absorbing state has not yet been characterized for single CdSe QDs, even conservative estimates based on ensemble measurements suggest that this shift is approximately an order of magnitude greater than the width of this state (17).

Under a range of electric fields, the peak shifts continuously over more than 60 meV (Fig. 1B). The slight change in zero-field energy over the series is due to spontaneous spectral diffusion (3, 12, 13). Shifts as large as 75 meV were observed in dots from this sample. These shifts are comparable to room-

Department of Chemistry, Massachusetts Institute of Technology, Cambridge, MA 02139.

*To whom correspondence should be addressed.

temperature linewidths (14), suggesting the potential for use in noncryogenic devices.

A plot of Stark shift as a function of field for this series (Fig. 1C) can be fit with the sum of a linear and quadratic function of field, indicating the presence of both polar and polarizable character in the emitting state

$$\Delta E = \mu\xi + \frac{1}{2}\alpha\xi^2 + \dots \quad (1)$$

where E is the energy of the transition, ξ is the applied electric field, and μ and α are projections of the excited-state dipole and polarizability, respectively, along the applied field (18). Although a polar component was suggested in ensemble absorption studies (10), Stark shifts in ensemble emission were found to be purely quadratic in the applied field (19). This finding is in contrast with our single dot observations.

A series of 11 consecutive spectra of the same single dot under different field conditions is shown in Fig. 2A. After an internal shift in the sixth frame due to spontaneous spectral diffusion, there is a clear increase in the magnitude of the response to a given applied field. The observed change is unlikely to be the result of QD reorientation on the substrate surface, which should be extremely slow at 10 K. In addition, similar changes were observed for dots embedded in a polymer matrix, where movement should be quenched.

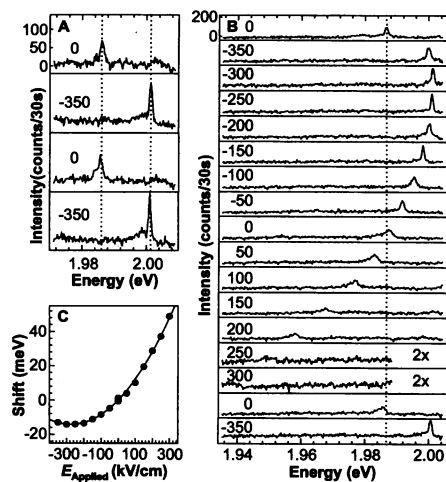


Fig. 1. Single QD Stark spectra. **(A)** Emission spectra of a single QD from the 37.5 Å ZnS-overcoated sample under conditions of alternating electric field. Frames indicate the applied field in kilovolts per centimeter. **(B)** Seventeen spectra of the same single dot under a range of electric fields. Frames indicate the applied field in kilovolts per centimeter and the magnification of the y axis. **(C)** Plot of Stark shift versus electric field for the spectra in (B). The line represents a fit to the sum of a linear and quadratic shift as a functions of field. The excitation intensity for all spectra in (A) and (B) was 25 W/cm².

In Fig. 2B, 100 consecutive spectra of the same dot are tabulated. Distinct changes in the zero-field position are observed. Accompanying each of these shifts is a corresponding change in the response to the applied field. The most dramatic change occurs at ~26 min, where the state changes from having a strong linear (dipole) component (shifts to both higher and lower energies) to having an extremely small or nonexistent linear component (shifts to lower energy under both field polarities). This does not mean that the excited-state dipole has disappeared, only that the component parallel to the applied field has decreased. The changes over time of the observed excited-state dipole, although not precluding contributions from an intrinsic asymmetry in structure or charge density in the ground state (20), shows that a significant portion of the excited-state dipole results from an extrinsic effect.

The data in Fig. 2 suggest a relation between spectral diffusion and the QCSE. Spectra in Fig. 3, A and B, demonstrate the similarities between shifts due to spectral diffusion and those induced by an applied electric field. An identical change in phonon coupling with shift characterizes both spectral diffusion and the single dot Stark effect (Fig. 3C). Phonon coupling is a measure of the overlap of electron and hole wave functions and should be sensitive to changes in polarization of the exciton. The observed similarities suggest that local electric fields are the cause of spectral diffusion.

Although an increase in the local electric field should result in a lower emission energy, there need not be a correlation between the direction of a spectral diffusion shift and the change in measured dipole moment along the applied external field. For example, in Fig. 2B the spectrum at 30 min is red-shifted from that at 22 min, suggesting a larger local field and therefore a larger total

induced dipole. However, the component of the dipole measured along the externally applied field is nearly nonexistent.

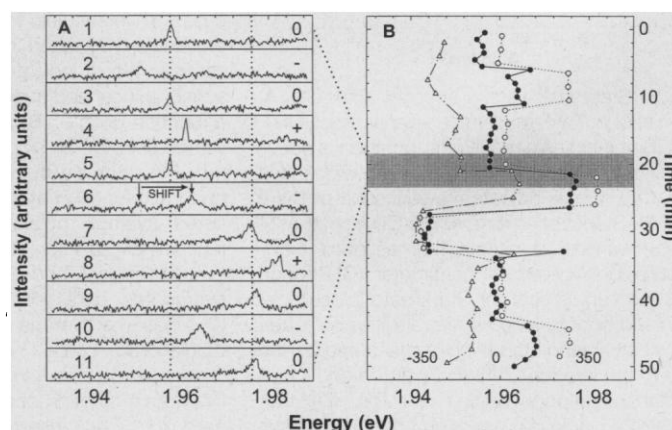
Within a given sample, we observed a range of values for both the polarizability and the excited-state dipole. Variations in polarizability may be due to differences in size, shape, and orientation of individual dots. Differences in the measured excited-state dipole are largely due to a distribution of dipole orientations relative to the applied field. A representative sample of four single dot Stark series from the 29 Å sample is plotted in Fig. 4A. Consistent with ensemble measurements (19), the average dipole component goes to zero over the distribution, yielding a net quadratic shift (Fig. 4B). From these data, an average polarizability of $\alpha = 2.38 \times 10^5 \text{ \AA}^3$ is obtained (with $\sigma = 1.37 \times 10^5 \text{ \AA}^3$ for the distribution). This value is comparable to the physical volume of the nanocrystallite ($\sim 10^5 \text{ \AA}^3$) and much larger than the polarizability of more traditional molecules (for anthracene $\alpha \approx 25 \text{ \AA}^3$). We can also extract the average magnitude of the excited-state dipole (88.3 Debye). This dipole is extremely large, comparable to an electron and hole separated by two-thirds of the nanocrystallite radius.

The observed, variable, excited-state dipole is consistent with a highly polarizable excited state in the presence of a strong, changing, local electric field:

$$\mu_{\text{ind}} = \alpha\xi_{\text{int}} \quad (2)$$

where ξ_{int} is the internal electric field resulting from any local fields, and μ_{ind} is the excited-state dipole induced by ξ_{int} . The magnitude of the internal field extracted in all samples ($\sim 10^5 \text{ V/cm}$) implies extensive state mixing near the band edge, with potentially serious implications regarding the current understanding of the electronic structure in these QDs (21). This conclusion has

Fig. 2. Influence of spectral diffusion on the QCSE of a single QD. **(A)** Eleven consecutive 30-s emission spectra of a single dot from the 37.5 Å ZnS-overcoated sample using a sequence of zero, negative, zero, positive electric fields. Frames indicate the spectrum number and the relative orientation of the field: (–) –350 kV/cm, (+) +350 kV/cm, and (0) 0 V/cm. **(B)** Summary of 100 consecutive 30-s spectra of the same dot under the field conditions described above. Data are plotted as a function of time, peak position, and electric field. Closed circles indicate zero field. Open triangles and open circles indicate fields of –350 and +350 kV/cm, respectively. The excitation intensity for all spectra was 25 W/cm².



also been reached on the basis of ensemble nonlinear optical techniques, where state mixing was observed directly (20).

The observed local electric fields may be the result of charge carriers on or near the surface of the QD. Photoionization has been proposed as the source of fluorescence intermittency in single CdSe QDs at room temperature (14). Photoionization leaves a charged QD core that may not relax radiatively upon further excitation. Emission resumes when the core is neutralized by the return of the ejected charge. A similar on-off behavior was observed at liquid helium temperatures (3, 13). At 10 K, however, there is little thermal energy to promote the return of an external charge. Instead, neutralization may occur through an additional ionization event, resulting in an emitting QD in the presence of a potentially large and randomly oriented local electric field.

The presence of such fields in ensemble samples represents an additional form of inhomogeneous broadening that will not be

eliminated by improvements in sample size and shape distribution. Instead, modifications of the ionization barrier (15), changes in the surrounding matrix, or both, may be required.

Additional ionization or recombination events, as well as relocalization of external charges, could result in changes in both the zero-field energy and the excited-state dipole of a single QD. This is consistent with the observations shown in Fig. 2. The magnitude of spectral diffusion shifts implies variations in the local field on the order of 10^5 to 10^6 V/cm (unscreened) and is consistent with the addition or removal of an electron from the surface of the QD.

Small fluctuations in the local field ($\Delta\xi_{\text{int}}$) may result from oscillations of an external charge between trap states. The resulting small spectral shifts have been implicated as a source of single QD line broadening (3). The total width of a spectral peak [$\Delta(\Delta E)$] is therefore dependent on the range over which the spectrum shifts in response to local field variations. The inherent squared dependence of the QCSE on electric field

$$\Delta E = \alpha(\xi_{\text{int}} + \xi_{\text{applied}})^2 \quad (3)$$

means that the width of a “spectral diffusion–broadened” peak will depend on the total field present:

$$\Delta(\Delta E) = 2\alpha(\xi_{\text{int}} + \xi_{\text{applied}})\Delta\xi_{\text{int}} \quad (4)$$

Under an applied field, shifts to higher energy (lower total field) should therefore be accompanied by narrower spectral peaks. This effect is clearly observed in Fig. 1B (22). The final frame of Fig. 1B shows that this broadening is a reversible effect of the electric field and not a degradation of the QD structure. A plot of peak width as a function of shift, taken from a subsequent voltage

series, reveals a roughly square root dependence, consistent with this model (Fig. 3D). A similar trend in peak width with shift resulting from spectral diffusion is not expected. In our model, spectral diffusion shifts arise from a change in the charge distribution around the QD. As a consequence, a change in the extent of $\Delta\xi_{\text{int}}$ may also be expected, and it is these local fluctuations that give rise to the observed linewidths. It is therefore not possible to predict the effect of a spectral diffusion shift on the linewidth of a single dot spectrum.

The increase in average polarizability with size (Fig. 4C) is consistent with ensemble measurements (19) and with the increase in volume of the QDs. The observed increase in excited-state dipole with size (Fig. 4D) is a result of the corresponding increase in polarizability. The internal electric field actually decreases with size (Fig. 4D). This result is consistent with an increase in the distance of an external charge from the center of the exciton wave function.

To reinforce this result, we also studied the 37.5 Å ZnS-overcoated sample. The measured values of the polarizability for the 37.5 Å standard and overcoated samples were statistically identical, consistent with minimal delocalization of the exciton into the ZnS shell (15). At the same time, a significant decrease in the excited-state dipole was observed. This result is consistent with the idea that the ZnS shell forces external charges to reside farther from the exciton wave function, while simultaneously screening local external fields and acting as a barrier to further ionization (14).

These electric field studies of single CdSe nanocrystallite QDs have revealed both polar and polarizable character in the lowest excited state. The polar component has been

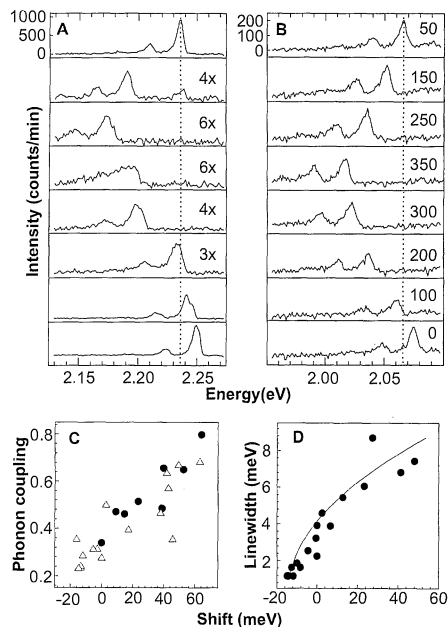
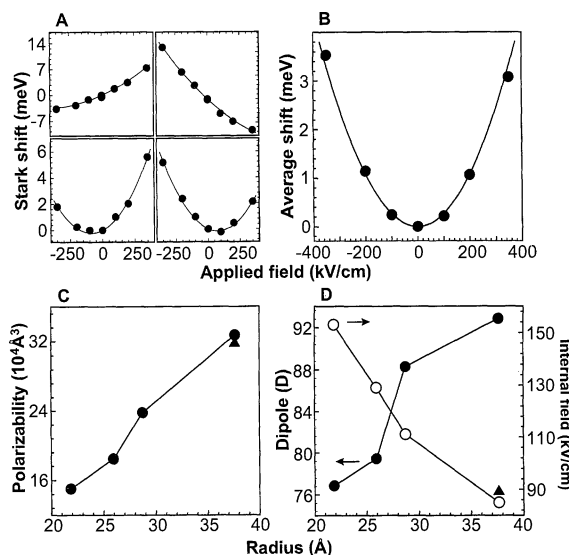


Fig. 3. Stark shift versus spectral diffusion. (A) Eight sequential 1-min emission spectra of a single QD shifting as a result of spontaneous spectral diffusion in the absence of an applied electric field (3). Frames indicate magnification of the y axis. (B) Stark series for a single QD from the 24 Å ZnS-overcoated sample. Frames indicate applied field in kilovolts per centimeter. (C) Phonon coupling versus shift for Stark data (closed circles) and spontaneous spectral diffusion (open triangles). Phonon coupling is measured as the ratio of the integrated intensity of the one longitudinal optical phonon line to the ZPL. (D) Line-width of a single dot emission spectrum versus shift from the zero-field position in response to an applied electric field. The excitation intensities for data in (A), (B), and (D) were 2500, 285, and 25 W/cm², respectively.

Fig. 4. Spectral response to an applied electric field. (A) Stark shift of emission versus field for four different single QDs taken from the 29 Å sample. Lines indicate fits to the sum of a linear and quadratic shift as a function of field. (B) Average shift versus field for 54 single QDs from the 29 Å sample with the fit to a pure quadratic function of field. (C) Measured average polarizability as a function of size for standard dots (closed circles) and 37.5 Å ZnS-overcoated dots (closed triangle). (D) Measured average excited-state dipole and internal electric field (closed and open circles, respectively) as a function of size for standard dots. The closed triangle indicates the average excited-state dipole for the 37.5 Å ZnS-overcoated dots. The excitation intensity for all data was 250 W/cm² (23).



attributed to an excited-state dipole moment, induced by the presence of local electric fields. These fields, which vary over time and produce spontaneous spectral diffusion, are thought to result, in part, from the presence of charge carriers on or near the QD surface.

REFERENCES AND NOTES

1. D. A. Miller, *Confined Excitons and Photons* (Plenum, New York, 1995), p. 675.
2. L. Brus, *Appl. Phys. A* **53**, 456 (1991); A. P. Alivisatos, *Science* **271**, 933 (1996).
3. S. A. Empedocles, D. J. Norris, M. G. Bawendi, *Phys. Rev. Lett.* **77**, 3873 (1996).
4. R. Leon, P. M. Petroff, D. Leonard, S. Fafard, *Science* **267**, 1966 (1995).
5. D. Gammon *et al.*, *ibid.* **277**, 85 (1997).
6. C. B. Murray, D. J. Norris, M. G. Bawendi, *J. Am. Chem. Soc.* **115**, 8706 (1993).
7. M. Danek *et al.*, *J. Cryst. Growth* **145**, 714 (1994).
8. C. R. Kagan *et al.*, *Phys. Rev. Lett.* **76**, 1517 (1996).
9. C. B. Murray, C. R. Kagan, M. G. Bawendi, *Science* **270**, 1335 (1995).
10. V. L. Colvin and A. P. Alivisatos, *J. Chem. Phys.* **97**, 730 (1992); V. L. Colvin, K. L. Cunningham, A. P. Alivisatos, *ibid.* **101**, 7122 (1994).
11. F. Hache, D. Richard, C. Flytzanis, *Appl. Phys. Lett.* **55**, 1504 (1989); A. Sacra, D. J. Norris, C. B. Murray, M. G. Bawendi, *J. Chem. Phys.* **103**, 5236 (1995).
12. S. A. Blanton, M. A. Hines, P. Guyot-Sionnest, *Appl. Phys. Lett.* **69**, 3905 (1996).
13. J. Tittel *et al.*, *J. Phys. Chem. B* **101**, 3013 (1997).
14. M. Nirmal *et al.*, *Nature* **383**, 802 (1996).
15. M. A. Hines and P. Guyot-Sionnest, *J. Phys. Chem.* **100**, 468 (1996); B. O. Dabbousi *et al.*, *J. Phys. Chem. B*, **101**, 9463 (1997).
16. Numerical calculations show a relatively uniform field across the substrate surface at a distance farther than 1 μm from either electrode (the field profile varies with $\sigma = 7\%$ of the mean).
17. D. Norris, Al. Efros, M. Rosen, M. Bawendi, *Phys. Rev. B* **53**, 16347 (1996).
18. Formally, what is measured in these experiments is actually the difference between the excited- and ground-state dipole (polarizability). For simplicity in discussion, we refer to this value as the excited-state dipole (polarizability). This is a reasonable assertion because, to a first approximation, any structural (ground-state) dipole (polarizability) should be relatively unaffected by the presence of a delocalized excitation.
19. A. Sacra, thesis, Massachusetts Institute of Technology (1996).
20. M. E. Schmidt, S. A. Blanton, M. A. Hines, P. Guyot-Sionnest, *J. Chem. Phys.* **106**, 5254 (1997).
21. Al. L. Efros *et al.*, *Phys. Rev. B* **54**, 1 (1996).
22. A similar broadening in QWs results from a lifetime effect due to field ionization of the exciton. If the observed broadening in CdSe QDs was lifetime-limited, implying an excited-state lifetime of $\sim 10^{-14}$ s, the very slow radiative relaxation ($\sim 10^{-6}$ s) would be completely quenched (quantum yield $\sim 10^{-8}$). The observed high fluorescence intensity suggests that field ionization is not a significant contribution.
23. Data were collected from 47 single QDs for the 37.5 Å overcoated sample and from 57, 83, 74, and 16 single QDs for the 37.5 Å, 29 Å, 26 Å, and 22 Å standard samples, respectively. Calculations included screening by the CdSe core and ZnS shell as necessary.
24. S.A.E. benefited from a Department of Defense graduate fellowship. This work was supported by the David and Lucile Packard Foundation and the Sloan Foundation. This research was funded in part by the NSF-Materials Research Science and Engineering Center program (DMR-94-00034). We thank the Massachusetts Institute of Technology Harrison Spectroscopy Laboratory (NSF-CHE-93-04251) for support and for allowing use of its facilities.

9 September 1997; accepted 3 November 1997

Natural Variation in a *Drosophila* Clock Gene and Temperature Compensation

Lesley A. Sawyer,* J. Michael Hennessy,*
Alexandre A. Peixoto,† Ezio Rosato, Helen Parkinson,
Rodolfo Costa, Charalambos P. Kyriacou‡

The threonine-glycine (Thr-Gly) encoding repeat within the clock gene *period* of *Drosophila melanogaster* is polymorphic in length. The two major variants (*Thr-Gly*)17 and (*Thr-Gly*)20 are distributed as a highly significant latitudinal cline in Europe and North Africa. Thr-Gly length variation from both wild-caught and transgenic individuals is related to the flies' ability to maintain a circadian period at different temperatures. This phenomenon provides a selective explanation for the geographical distribution of Thr-Gly lengths and gives a rare glimpse of the interplay between molecular polymorphism, behavior, population biology, and natural selection.

The clock gene *period* (*per*) in *Drosophila melanogaster* is an essential component of circadian rhythmicity, and its product is involved in a negative autoregulatory feedback loop with the Timeless protein [reviewed in (1)]. The *per* gene has a repetitive region, which encodes alternating pairs of predominantly threonine-glycine, but also serine-glycine dipeptide pairs (2). This repetitive region is conserved in the mammalian *per* homolog, suggesting that it may play an important functional role in circadian phenotypes (3). However, the only role assigned for the Thr-Gly region is to convey the species-specific characteristics of the ultradian male courtship song cycle (4).

Within natural populations of *D. melanogaster* and *D. simulans*, the Thr-Gly repeat is polymorphic in length (5). In *D. melanogaster*, Thr-Gly alleles that encode 14, 17, 20, and 23 dipeptide pairs [termed (*Thr-Gly*)14, (*Thr-Gly*)17, and so on] make up about 99% of European variants (6). The (*Thr-Gly*)17 and (*Thr-Gly*)20 alleles are distributed as a highly significant latitudinal cline, with high occurrences of the former observed in the southern Mediterranean and the latter predominating in northern Europe (6). In both *D. melanogaster* and *D. simulans*, analyses of intraspecific Thr-Gly haplotypes aimed at testing neutral models suggest that the repetitive regions are under selection (7, 8). Furthermore, several stud-

ies revealed that Thr-Gly repeat length evolves with the immediate flanking amino acids (9, 10). If selection is shaping variation in the repetitive region, then the Thr-Gly cline in Europe implicates temperature as a possible selective agent.

Therefore, we studied the temperature responses of natural Thr-Gly length variants, which have the sequences shown in Fig. 1 (11). For simplicity, the (*Thr-Gly*)17c allele, which has the downstream (Thr-Gly)2 deletion, is referred to as (*Thr-Gly*)15. The Ser-to-Phe replacement is the only amino acid polymorphism that has been encountered in the immediate flanking regions surrounding the repeat in European (11) and other populations (12).

Free-running circadian locomotor activity rhythms of males from 37 different attached-X lines, whose *per*-carrying X chromosomes originated from eight European and North African localities, were examined at 18° and 29°C (Table 1) (13). A further attached-X line whose original male carried the (*Thr-Gly*)23 allele from the American Canton-S laboratory strain was also added. This Thr-Gly haplotype is also found in European populations (11). The results based on spectral analysis (14) are presented in Table 1 and Fig. 2, A and B. Similar results were obtained with autocorrelation (Table 1) (15), but are not presented in detail. Two-way analysis of variance (ANOVA), performed with the 38 lines and temperature as the variables, gave significant Line and Temperature \times Line interactions ($P < 0.01$), and further ANOVA of the data pooled into genotypes also gave significant Genotype and Temperature \times Genotype interaction (both $P < 0.001$). Planned comparisons revealed that six of the 38 lines showed significant period differences between the two temperatures, whereas nine were significantly different when periods were determined with autocorrelation (Ta-

L. A. Sawyer, J. M. Hennessy, A. A. Peixoto, E. Rosato, H. Parkinson, C. P. Kyriacou, Department of Genetics, University of Leicester, LE1 7RH, UK.
R. Costa, Dipartimento di Biologia, Università di Padova, Via Trieste 75, 35121 Padova, Italy.

*These authors contributed equally to this work.

†Present address: Departamento de Bioquímica e Biologia Molecular Fundacao Oswaldo Cruz, Avenue Brasil, 4365-Manquinhos, CEP 21045-900, Rio de Janeiro, Brazil.

‡To whom correspondence should be addressed. E-mail: cpk@leicester.ac.uk